DOI: 10.1021/cg900336r

CRYSTAL GROWTH & DESIGN Article

2009, Vol. 9
4091–4095

A Novel Nonlinear Optical Crystal $Bi_2ZnOB_2O_6$

Feng Li,[†,‡] Shilie Pan,*[,†] Xueling Hou,[†] and Jun Yao[§]

[†]*Xinjiang Key Laboratory of Electronic Information Materials and Devices, Xinjiang Technical Institute of Physics & Chemistry, Chinese Academy of Sciences, Urumqi 830011, China,* [‡]*Graduate University of Chinese Academy of Sciences, Beijing 100049, China, and* [§]*State Key Laboratory of Optical Technologies for MicroFabrication & MicroEngineering, Institute of Optics and Electronics, Chinese Academy of Sciences, Chengdu 610209, China*

Received March 24, 2009; Revised Manuscript Received June 9, 2009

ABSTRACT: Sizable single crystals of a nonlinear optical (NLO) material, $Bi_2ZnOB_2O_6$, were grown by the Kyropoulos method from stoichiometric ratio compound melt. It is a congruent melting compound and crystallizes in the orthorhombic system, space group *Pba*2. The morphologies and habits of $Bi_2ZnOB_2O_6$ crystals grown using [100], [010], and [001] seeds were studied. The SHG efficiency of $Bi_2ZnOB_2O_6$ is 3−4 times that of KDP (KH_2PO_4). Its birefringence is pretty large (0.085−0.106). The experiments prove that $Bi_2ZnOB_2O_6$ crystal is nonhygroscopic and excellently deliquescence resistant.

Introduction

Nonlinear optical (NLO) materials have been playing an increasingly important role in laser science and technology.[1,2] Even though intensive efforts in the field have been made for about 40 years, it is still very attractive to search for new nonlinear optical materials with various practical interests.[3−5] Because of the broad transparent region, high damage threshold and moderate birefringence, borate crystals are one kind of important NLO materials for near-infrared (IR) through the visible to the ultraviolet (UV), and vacuum-UV (VUV) spectral regions, such as β-BaB_2O_4 (β-BBO), LiB_3O_5 (LBO), CsB_3O_5 (CBO), $CsLiB_6O_{10}$ (CLBO), $KBe_2BO_3F_2$ (KBBF), and BiB_3O_6 (BIBO).[6−11] Each class of crystals has not only advantages but also restrictions, such as very long growth period, serious hygroscopy, and layer growth habit. Many other new NLO crystals have come forth this decade,[12−23] but crystals with easy growth character, good physicochemical properties, and simple post-treatment process features are limited today. Considering the excellent qualities of borate, especially the BO_3 anionic group for NLO effect, we believe that there are many new promising NLO materials in complex borates and found $Bi_2ZnOB_2O_6$ in the end.

J. Barbier et al. reported $Bi_2ZnB_2O_7$ compound in 2005.[24] M. Li et al. prepared $Bi_2ZnB_2O_7$ with size $0.4 \times 0.4 \times 0.5$ mm^3 by solid-state reactions in 2007.[25] In researching on the $Bi_2O_3-ZnO-B_2O_3$ system,[26] we found that $Bi_2ZnB_2O_7$ ($Bi_2ZnOB_2O_6$) melts congruently and is an oxy-borate, which can be formulated as $Bi_2ZnOB_2O_6$. In this paper, we report crystal growth of $Bi_2ZnOB_2O_6$ along different directions from stoichiometric melt, its optical properties, and stability.

Experimental Procedures

Synthesis and Crystal Growth. A powder sample of $Bi_2ZnOB_2O_6$ was prepared by solid-state reaction techniques and examined by X-ray powder diffraction analysis. A stoichiometric ratio of Bi_2O_3, ZnO, and H_3BO_3 (all of analytical grade) was mixed thoroughly.

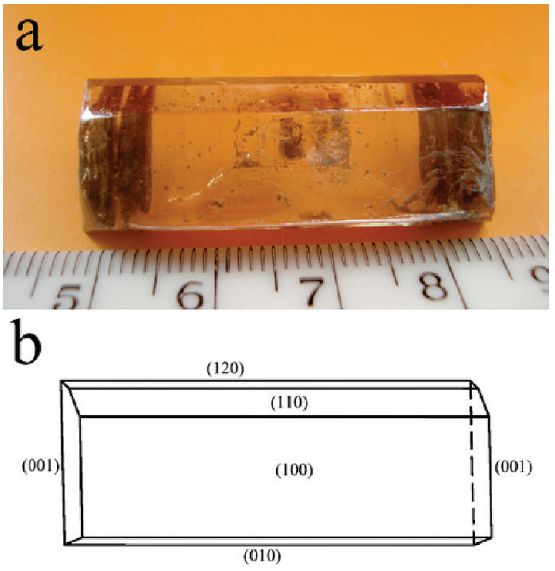

Figure 1. (a) Photo and (b) morphology of the $Bi_2ZnOB_2O_6$ crystal grown along the [100] direction.

The mixture was heated at 450 °C for 4 h and at 600 °C for 40 h. The material was ground between all heatings. A single-phase powder of $Bi_2ZnOB_2O_6$ was obtained when repeated heat treatment caused no further changes in the X-ray powder diffraction pattern.

$Bi_2ZnOB_2O_6$ single crystal was grown by the Kyropoulos method[27] from stoichiometric ratio compound melt. The powder samples were melted in a platinum crucible with 50 mm diameter and 40 mm height. The melting point of $Bi_2ZnOB_2O_6$ is 692 °C. The growth furnace was quickly heated to 800 °C, kept at that temperature for 20 h to ensure complete melting and homogeneity of the raw materials, and then quickly cooled to 692 °C. In the first run of growth, a platinum rod was dipped into the melt rapidly, and the temperature was reduced at a rate of 1 °C /h. The obtained crystals were branchy with inclusions, but parts of them were usable as seeds. After several growth experiments, suitable seed crystals were obtained. To study the growth habits of $Bi_2ZnOB_2O_6$ crystal, we used seed crystals with different directions ([100], [010], and [001]). Transparent $Bi_2ZnOB_2O_6$ crystals, shown in Figures 1−3, with sizes of 38 mm × 15 mm × 8 mm, 43 mm × 16 mm × 9 mm, and 34 mm × 25 mm × 7 mm, were obtained.

*Corresponding author. Address: Xinjiang Technical Institute of Physics & Chemistry, Chinese Academy of Sciences, 40-1 South Beijing Road, Urumqi 830011, China. Phone: (86)991-3674558. Fax: (86)991-3838957. E-mail: slpan@ms.xjb.ac.cn.

Published on Web 07/06/2009

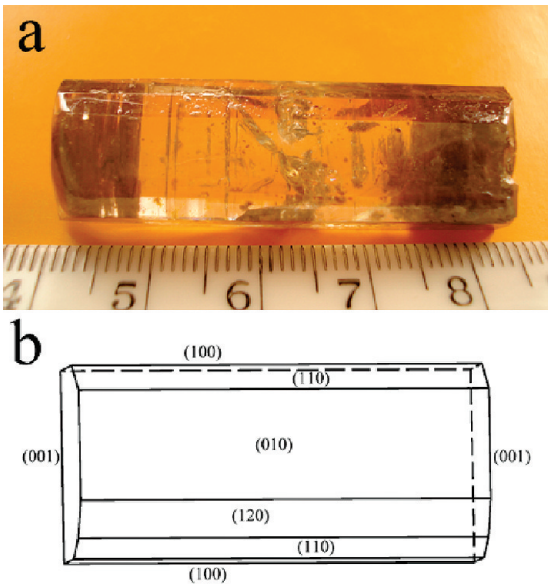

Figure 2. (a) Photo and (b) morphology of the $Bi_2ZnOB_2O_6$ crystal grown along the [010] direction.

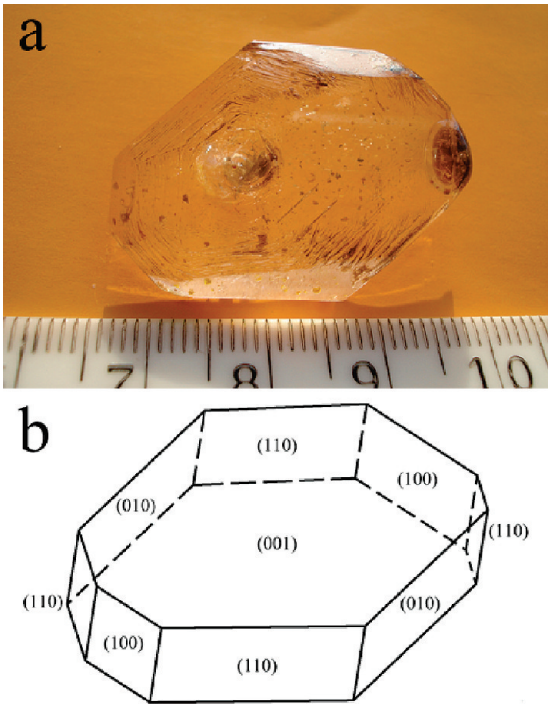

Figure 3. (a) Photo and (b) morphology of the $Bi_2ZnOB_2O_6$ crystal grown along the [001] direction.

X-ray Crystallography. X-ray powder diffraction analysis for $Bi_2ZnOB_2O_6$ was performed with a Bruker D8 ADVANCE X-ray diffractometer with graphite monochromatized Cu $K\alpha$ radiation. Table 1 presents the X-ray powder diffraction data of $Bi_2ZnOB_2O_6$. The crystal structure of $Bi_2ZnOB_2O_6$ was investigated using a Rigaku Saturn CCD diffractometer. The experimental parameters for data collection and refinement are given in Table 2. A numerical absorption correction was applied. The structure was solved with Shelxs-97 by the direct method and refined by full-matrix least-squares techniques with anisotropic thermal parameters for all atoms. The Flack absolute structure parameter[28] was estimated. Further details of the crystal structure investigation may be obtained from the CIF file in the Supporting Information.

Table 1. X-ray Powder Diffraction Data of $Bi_2ZnOB_2O_6$

h k l	d_{calcd}	d_{obsd}	I/I_0	*h k l*	d_{calcd}	d_{obsd}	I/I_0
0 0 1	4.8844	4.8762	40.6	1 3 2	1.9985	1.9984	21.0
2 2 0	3.8602	3.8541	24.4	3 1 2	1.9891	1.9872	20.1
0 2 1	3.6545	3.6484	6.7	2 3 2	1.9036	1.9023	4.7
2 0 1	3.6259	3.6216	7.8	3 5 0	1.8803	1.8799	11.9
1 3 0	3.4773	3.4717	27.3	5 3 0	1.8647	1.8639	14.6
3 1 0	3.4285	3.4243	30.0	0 4 2	1.8272	1.8273	7.1
2 2 1	3.0281	3.0257	100.0	6 0 0	1.8038	1.8025	8.8
1 3 1	2.8328	2.8294	54.4	3 5 1	1.7548	1.7540	11.3
3 1 1	2.8062	2.8031	51.8	5 3 1	1.7421	1.7411	21.9
0 4 0	2.7540	2.7516	7.1	4 2 2	1.7220	1.7209	10
4 0 0	2.7057	2.7027	11.3	6 0 1	1.6921	1.6915	17.8
2 3 1	2.5800	2.5787	3.9	3 4 2	1.6301	1.6289	7.5
0 0 2	2.4422	2.4415	18.7	5 4 1	1.6071	1.6075	9.0
4 2 0	2.4285	2.4276	11.4	2 5 2	1.5659	1.5663	4.2
1 4 1	2.3421	2.3411	4.7	2 2 3	1.5002	1.4999	11.0
4 1 1	2.3140	2.3120	4.8	3 5 2	1.4899	1.4896	9.4
4 2 1	2.1746	2.1741	7.4	3 1 3	1.4707	1.4707	8.5
2 2 2	2.0638	2.0632	11.3	4 6 1	1.4507	1.4507	7.9

Table 2. Crystal Data and Structure Refinement for $Bi_2ZnOB_2O_6$

empirical formula	$Bi_2ZnOB_2O_6$
fw	616.95
wavelength	0.71073 Å
cryst syst	orthorhombic
space group	*Pba*2
a (Å)	10.823(2)
b (Å)	11.016(2)
c (Å)	4.8844(9)
V (Å^3)	582.39(19)
Z	4
density (calcd) (Mg/m^3)	7.036
absorp coeff (mm^{-1})	64. 356
cryst size (mm^3)	0.10 × 0.10 × 0.03
theta range for data collection (deg)	2.46−30.47
refinement method	full-matrix least-squares on F^2
GOF on F^2	1.090
final *R* indices [$F_o^2 > 2\sigma(F_o^2)$][a]	R_1 = 0.0394, wR_2 = 0.0983
R indices (all data)[a]	R_1 = 0.0421, wR_2 = 0.0993
largest diff. peak and hole	4.892 and −3.336 e Å^{-3}

[a] $R_1 = \Sigma||F_o| - |F_c||/\Sigma|F_o|$ and $wR_2 = [\Sigma w(F_o^2 - F_c^2)^2/\Sigma wF_o^4]^{1/2}$ for $F_o^2 > 2\sigma(F_o^2)$.

IR Spectroscopy. IR spectroscopy was carried out with the objective of specifying and comparing the coordination of boron in $Bi_2ZnOB_2O_6$ compound. The mid-infrared spectrum was obtained at room temperature via a BRUKER EQUINOX 55 Fourier transform infrared spectrometer. The sample was mixed thoroughly with dried KBr. The spectrum was collected in a range from 400 to 4000 cm^{-1} and shown in Figure S1 in the Supporting Information.

Transmittance Spectra. The transmittance spectra of $Bi_2ZnOB_2O_6$ crystal were measured by a Perkin-Elmer Lambda 900 UV/vis/NIR spectrophotometer and a BRUKER EQUINOX 55 Fourier transform infrared spectrometer, respectively and shown in Figure 4. It can be seen that a wide transmission range is observed from 330 to 3750 nm.

Second Harmonic Generation Measurement. The measurement of the powder frequency-doubling effect was carried out on the sieved (55−88 mesh) powder sample of $Bi_2ZnOB_2O_6$ by means of the modified method of Kurtz and Perry.[29] The fundamental wavelength is 1064 nm generated by a Q-switched Nd:YAG laser (10 kHz, 10 ns). The SHG wavelength is 532 nm. KDP (KH_2PO_4) and LBO (LiB_3O_5) powders sieved (55−88 mesh) were used as references to estimate the relative SHG efficiency.

Refractive Indices. The refractive indices of $Bi_2ZnOB_2O_6$ were measured at ten discrete wavelengths in a wavelength range from 404.7 to 694.3 nm by the minimum-deviation method. $Bi_2ZnOB_2O_6$ belongs to orthorhombic crystal system and has a space group of *Pba*2, so two prisms are needed to measure all of its refractive indices. As shown in Figure 5a, two prisms were cut and polished with vertex angle of 20°. The crystal faces are denoted in Figure 5b.

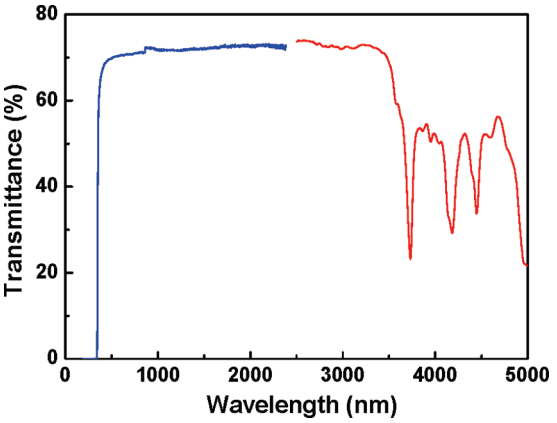

Figure 4. Transmittance curves of $Bi_2ZnOB_2O_6$ crystal.

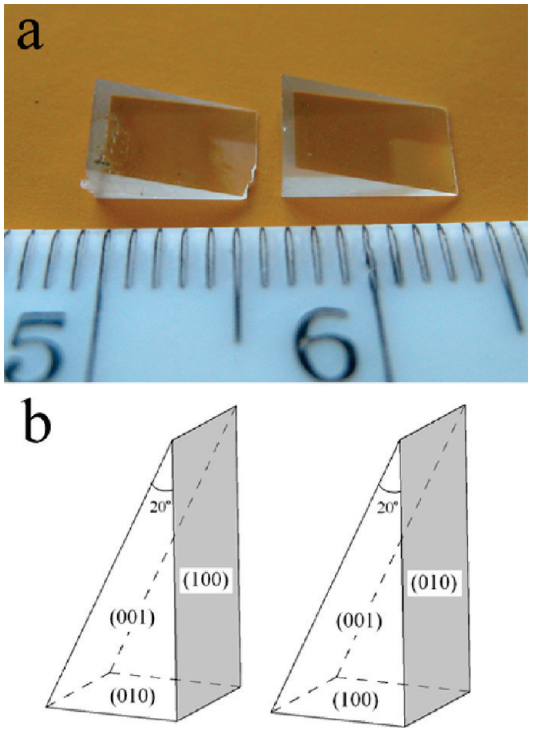

Figure 5. (a) Photo and (b) morphology of the $Bi_2ZnOB_2O_6$ crystal prisms.

Antideliquescence and Stability Test. A crystal sample with size of $5 \times 4 \times 2$ mm^3 was cut along phase matching (PM) direction from as-grown $Bi_2ZnOB_2O_6$ crystal. The incident and exist surface were polished. The sample without any other treatment and protection was then placed in water and irradiated by a Q-switched Nd:YAG laser.

Results and Discussion

$Bi_2ZnOB_2O_6$ crystallizes in the noncentrosymmetric orthorhombic space group *Pba*2. The structure is shown in Figure 6. Two unique bismuth atoms, one unique zinc atom, two boron atoms, and seven oxygen atoms are in the asymmetric unit. The basic building units of the title compound are trigonal planar BO_3 and tetrahedron BO_4, which form isolated B_2O_5 and B_2O_7, respectively. The dimers that connected with ZnO_4 tetrahedra form infinite sheets, whereas Bi^{3+} cations form another sheets. The two kinds of sheets alternate with each other along *c* axis forming the extended framework of the crystal structure.

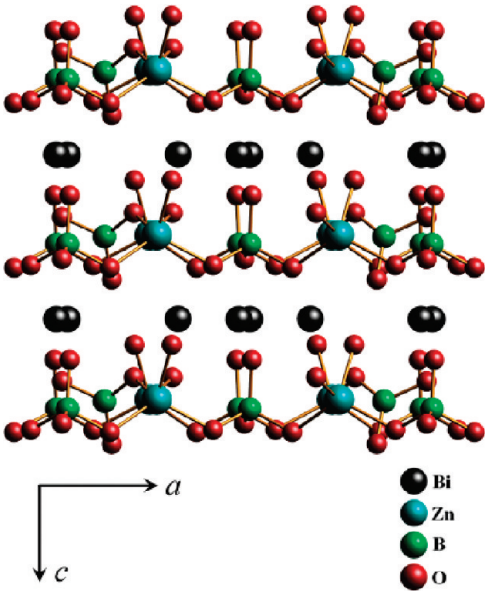

Figure 6. Drawing of the structure of $Bi_2ZnOB_2O_6$ viewed along the *b* axis.

The crystal of $Bi_2ZnOB_2O_6$ can be easily grown because of not only its congruent melting nature but also its low viscosity and low melting point. Figure 1a presents the photo of $Bi_2ZnOB_2O_6$ crystal with the seed crystal oriented along [100] direction, whereas Figure 1b shows the morphology and face indices. The crystal growth temperature was a little lower than its freezing point at the first day, and then lowered 0.8 °C at the second day for improving growth rate. From the photo, we can see that there are clear boundaries that divide the crystal into three parts. The middle section is transparent, whereas the outside parts have many inclusions. Figure 2 presents the photo of $Bi_2ZnOB_2O_6$ crystal with the seed crystal oriented along the [010] direction, which is very similar to Figure 1. Figure 3 shows the $Bi_2ZnOB_2O_6$ crystal with the seed crystal oriented along the [001] direction. There are many differences between the crystals grown along [100], [010], and [001], though the growth conditions are similar. There are no evident boundary in the [001] crystal, and almost no inclusions except some crystal growth striae. Moreover, the growth periods of [001] crystal shown in Figure 3 was about 3 days, whereas the periods of [100] crystal and [010] crystal shown in Figures 1 and 2 were no more than 2 days. Obviously, the growth rates of $Bi_2ZnOB_2O_6$ crystal along different directions at the same temperature are different. The [001] direction has a higher growth rate than the [100] and [010] directions. In addition, it is easier to introduce inclusions along the [001] direction when the growth rate is too high. In Figure 3, the morphological faces are (001), (100), (010), (110), and (120), which can also be found in Figures 1 and 2, and we find no other faces in all of the present experiments.

The compound crystallizes in a noncentrosymmetric space group, a basic condition for a potential harmonic generation material. According to the anionic group theory,[30] the nonlinearity of a borate crystal originates in the boron−oxygen groups. In fact, $Bi_2ZnOB_2O_6$ was found to have a powder SHG effect about 3−4 times that of KDP and a little larger than that of LBO. The nonlinear optical coefficients determined by the Maker fringes method at 1064 nm are $d_{31} = 2.46d_{36}$ (KDP), $d_{32} = 7.64d_{36}$ (KDP), and $d_{33} = 2.62d_{36}$ (KDP).

Table 3. Refractive Indices of $Bi_2ZnOB_2O_6$ Crystal

λ (μm)	n_x	n_y	n_z	$n_z - n_x$
0.4047	2.1777	2.2140	2.2840	0.1063
0.4078	2.1744	2.2107	2.2799	0.1055
0.4358	2.1475	2.1846	2.2489	0.1014
0.4861	2.1151	2.1525	2.2103	0.0952
0.4916	2.1122	2.1498	2.2068	0.0946
0.5461	2.0904	2.1278	2.1810	0.0906
0.5770	2.0811	2.1184	2.1703	0.0892
0.5893	2.0778	2.1152	2.1663	0.0885
0.6563	2.0637	2.1009	2.1498	0.0861
0.6943	2.0574	2.0947	2.1427	0.0853

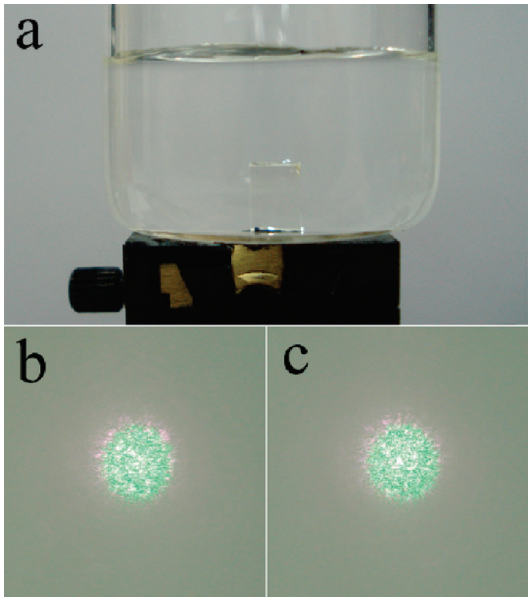

Figure 7. SHG test in water. (a) Photo of the $Bi_2ZnOB_2O_6$ crystal sample in water. (b) Green light (frequency-doubled output) plot on the screen emitted from the crystal sample in water. (c) Green light plot 2 days later.

The values of room-temperature refractive indices measured at specific wavelengths are summarized in Table 3. Assignment of dielectric and crystallographic axes is X, Y, $Z \Rightarrow b$, c, a assuming $n_x < n_y < n_z$, shown in Figure S2 in the Supporting Information. The experimental data were fitted using Sellmeier equations and shown as follows

$$n_x^2 = 4.04925 + 0.08002767/(\lambda^2 - 0.04815881)$$

$$n_y^2 = 4.19639 + 0.08387125/(\lambda^2 - 0.04473102)$$

$$n_z^2 = 4.36860 + 0.09624239/(\lambda^2 - 0.05022927)$$

where the wavelength, λ, is in micrometers. The birefringence of $Bi_2ZnOB_2O_6$ is pretty large (0.085−0.106). The result indicates that $Bi_2ZnOB_2O_6$ belongs to positive biaxial optical crystal and predicts that the PM angle for type I SHG of 1064 nm in XY plane is $\theta = 90°$ and $\varphi = 49°$ (see Figure S2 in the Supporting Information). The shortest wavelength achieved by SHG based on the Sellmeier equations is 485 nm.

A crystal sample was prepared along the PM direction ($\theta = 90°$, $\varphi = 49°$) and irradiated by a Q-switched Nd:YAG solid-state laser (1064 nm, 10 kHz, 10 ns). An intense green light (frequency-doubled output) was emitted from the sample and projected onto a screen. To test the deliquescence of $Bi_2ZnOB_2O_6$ crystal, we then put the crystal sample without any treatment and protection into a beaker with water at room temperature as shown in Figure 7a. The incident radiation passed through water and irradiated the sample. The green light that emitted from the sample, that also passed through water was almost the same (shown in Figure 7b), and the green light spot on the screen had no observable change while the sample was kept in water for 2 days (see Figure 7c). Obviously, $Bi_2ZnOB_2O_6$ crystal has excellent deliquescence resistance and is very stable in the air even if in a moist environment.

Conclusions

$Bi_2ZnOB_2O_6$ is a new kind of congruent melting oxy-borate with the structure of a three-dimensional network consisting of $ZnB_2O_7^{6-}$ layers alternating with octahedrally coordinated Bi^{3+} cations along the c axis. $Bi_2ZnOB_2O_6$ crystals have been grown by the Kyropoulos method[27] from stoichiometric ratio compound melt along [100], [010], and [001] directions. The [001] orientation (along c axis) is a better growth direction. The SHG effect of $Bi_2ZnOB_2O_6$ is about 3−4 times that of KDP. $Bi_2ZnOB_2O_6$ belongs to positive biaxial optical crystal and has large birefringence. $Bi_2ZnOB_2O_6$ also has stable chemical properties, especially very good antideliquescence. All these excellent characters of $Bi_2ZnOB_2O_6$ crystal make it a promising candidate for NLO materials.

Acknowledgment. The authors gratefully acknowledge the financial support from the Natural Science Foundation of Xinjiang Uygur Autonomous Region of China (Grant 200821159), the National Natural Science Foundation of China (Grant 50802110), the "High Technology Research and Development Program" of Xinjiang Uygur Autonomous Region of China (Grant 200816120), the Excellent "One Hundred Talented People" of the Chinese Academy of Sciences (CAS), the West Light Foundation of the CAS, and the CAS Special Grant for Postgraduate Research, Innovation and Practice.

Supporting Information Available: IR spectrum, Assignment of dielectric and crystallographic axis and X-ray crystallographic information file (CIF) for $Bi_2ZnOB_2O_6$. This information is available free of charge via the Internet at http://pubs.acs.org.

References

(1) Cyranoski, D. *Nature* **2009**, *457*, 953.
(2) Chen, C.; Lin, Z.; Wang, Z. *Appl. Phys. B: Laser Opt.* **2005**, *80*, 1.
(3) Sasaki, T.; Mori, Y.; Yoshimura, M.; Yap, Y. K.; Kamimura, T. *Mater. Sci. Eng., R* **2000**, *30*, 1.
(4) Chen, C.; Wang, Y.; Wu, B.; Wu, K.; Zeng, W.; Yu, L. *Nature* **1995**, *373*, 322.
(5) Becker, P. *Adv. Mater.* **1998**, *10*, 979.
(6) Ye, N.; Tang, D. *J. Cryst. Growth* **2006**, *293*, 233.
(7) Chen, C.; Wu, Y.; Jiang, A.; Wu, B.; You, G.; Li, R.; Lin, S. *J. Opt. Soc. Am. B* **1989**, *6*, 616.
(8) Wu, Y.; Sasaki, T.; Nakai, S.; Yokotani, A.; Tang, H.; Chen, C. *Appl. Phys. Lett.* **1993**, *62*, 2614.
(9) Pan, S.; Wu, Y.; Fu, P.; Wang, X.; Zhang, G.; Chen, C. *J. Opt. Soc. Am. B* **2004**, *21*, 761.
(10) Chen, C.; Wu, B.; Jiang, A.; You, G. *Sci. Sin. B* **1985**, *28*, 235.
(11) Hellwig, H.; Libertz, J.; Bohaty, L. *Solid State Commun.* **1999**, *109*, 249.
(12) Pan, S.; Smit, J. P.; Watkins, B.; Marvel, M. R.; Stern, C. L.; Poeppelmeier, K. R. *J. Am. Chem. Soc.* **2006**, *128*, 11631.
(13) Norquist, A. J.; Heier, K. R.; Halasyamani, P. S.; Stern, C. L.; Poeppelmeier, K. R. *Inorg. Chem.* **2001**, *40*, 2015.
(14) Hu, Z.; Yoshimura, M.; Mori, Y.; Sasaki, T. *J. Cryst. Growth* **2004**, *260*, 287.
(15) Aka, G.; Kahn-Harari, A.; Vivien, D.; Benitez, J.-M.; Salin, F.; Godard, J. *Eur. J. Solid State Inorg. Chem.* **1996**, *33*, 727.

(16) Yuan, X.; Shen, D.; Wang, X.; Shen, G. *J. Cryst. Growth* **2006**, *292*, 458.
(17) Muller, E. A.; Cannon, R. J.; Sarjeant, A. N.; Ok, K. M.; Halasyamani, P. S.; Norquist, A. J. *Cryst. Growth Des.* **2005**, *5*, 1913.
(18) Pan, S.; Wu, Y.; Fu, P.; Zhang, G.; Li, Z.; Du, C.; Chen, C. *Chem. Mater.* **2003**, *15*, 2218.
(19) Kong, F.; Jiang, H.; Hu, T.; Mao, J. *Inorg. Chem.* **2008**, *47*, 10611.
(20) Penin, N.; Seguin, L.; Gérand, B.; Touboul, M.; Nowogrocki, G. *J. Alloys Compd.* **2002**, *334*, 97.
(21) Egorova, B. V.; Olenev, A. V.; Berdonosov, P. S.; Kuznetsov, A. N.; Stefanovich, S. Y.; Dolgikh, V. A.; Mahenthirarajah, T.; Lightfoot, P. *J. Solid State Chem.* **2008**, *181*, 1891.
(22) Wang, J.; Zhang, C.; Liu, Y.; Zhang, J.; Hu, X.; Jiang, M. *J. Mater. Res.* **2003**, *18*, 2478.
(23) Wang, G.; Wu, Y.; Fu, P.; Liang, X.; Xu, Z.; Chen, C. *Chem. Mater.* **2002**, *14*, 2044.
(24) Barbier, J.; Penin, N.; Cranswick, L. M. *Chem. Mater.* **2005**, *17*, 3130.
(25) Li, M.; Chen, X.; Chang, X.; Zang, H.; Xiao, W. *J. Syn. Cryst.* **2007**, *36*, 1005.
(26) Zargarova, M. I.; Kasumova, M. F.; Abdullaev, G. K. *Russ. J. Inorg. Chem.* **1987**, *32*, 737.
(27) Kyropoulos, S. *Z. Anorg. Chem.* **1926**, *154*, 308.
(28) Flack, H. D. *Acta Crystallogr., Sect. A* **1983**, *39*, 876.
(29) Kurtz, S. K.; Perry, T. T. *J. Appl. Phys.* **1968**, *39*, 3798.
(30) Chen, C.; Wu, Y.; Li, R. *Int. Rev. Phys. Chem.* **1989**, *8*, 65.